

# Rare earth element characteristics of pyrope garnets from the Kaavi-Kuopio kimberlites – implications for mantle metasomatism



MARJALEENA LEHTONEN

*Geological Survey of Finland, P.O. Box 96, FIN-02151 Espoo, Finland*

## Abstract

Peridotitic garnet xenocrysts from five kimberlite pipes in the Kaavi-Kuopio area of eastern Finland have been studied using major and trace element geochemistry to obtain information on the stratigraphy, compositional variability and evolutionary history of the underlying lithospheric mantle. Ni thermometry on garnet xenocrysts gives 650–1350°C and, when extrapolated to the geotherm determined using mantle xenoliths, indicates a sampling interval of c. 80–230 km. Three distinct mantle layers are recognized based on the xenolith/xenocryst record: (1) A shallow, <110 km, garnet-spinel peridotite layer characterized by distinctive “CCGE” pyropes. (2) A variably depleted lherzolitic and harzburgitic horizon from 110 to 180 km. (3) A deep layer, >180 km, composed largely of fertile material. The chondrite-normalized REE profiles of subcalcic harzburgitic garnet xenocrysts originating from layer 2 bear evidence of an extensive ancient melt extraction event, similar to that observed in lithosphere underlying Archean cratons elsewhere. Memory of this event has possibly also been preserved in the REE<sub>N</sub> signatures of rare depleted garnets from layer 3 and in the CCGE pyropes from layer 1 despite their saturation in Ca. The lherzolitic and megacryst garnet varieties exhibit LREE<sub>N</sub> depletion relative to MREE<sub>N</sub> and HREE<sub>N</sub>, with the steady enrichment from Sm<sub>N</sub> to Yb<sub>N</sub> typical of Ca-saturated mantle garnets. The enrichment of MREE and HREE probably derives from a metasomatic event caused by silicate melts close in composition to megacryst magma, which also imprinted a Ti-metasomatic overprint on many pyrope garnets. Harzburgitic and rare lherzolitic garnets, however, appear to have escaped this metasomatism.

---

**Key words:** mantle, kimberlite, garnet group, xenocrysts, peridotites, xenoliths, geochemistry, rare earths, geologic thermometry, Kaavi, Kuopio, Finland

---

e-mail: marja.lehtonen@gtk.fi

## 1. Introduction

The Kaavi-Kuopio Kimberlite Province situated at the Karelian craton margin contains at least nineteen kimberlites with mineralogy typical of Group I kimberlite (Tyni, 1997; O'Brien & Tyni, 1999). The pipes have intruded Archean (3.5–2.6 Ga) basement gneisses and allochthonous Proterozoic (1.9–1.8 Ga) metasediments thrust onto the craton during the Svecofennian orogeny (Kontinen et al., 1992; Fig. 1). Several methods have been used to date the kimberlite magmatism (Tyni, 1997; Peltonen et al., 1999; Peltonen & Mänttari, 2001) but the U-Pb ion probe ages of 589–626 Ma from perovskites (O'Brien et al., 2005) are considered to be the most reliable.

Mantle xenoliths and xenocrysts from the Kaavi-Kuopio pipes have been studied by Peltonen (1999), Peltonen et al. (1999), Woodland & Peltonen (1999) and Lehtonen et al. (2004). A geotherm corresponding to a  $36 \text{ mW/m}^2$  has been calculated using heat flow constraints and xenolith modes, thermobarometry and thermal properties (Kukkonen & Peltonen, 1999; Kukkonen et al., 2003). The xenolith/xenocryst suite provides evidence of vertical compositional variability of the lithospheric mantle adjacent to the ancient suture zone between the Archean Karelian craton and the Proterozoic Svecofennian mobile belt, with at least three distinct mantle horizons identified

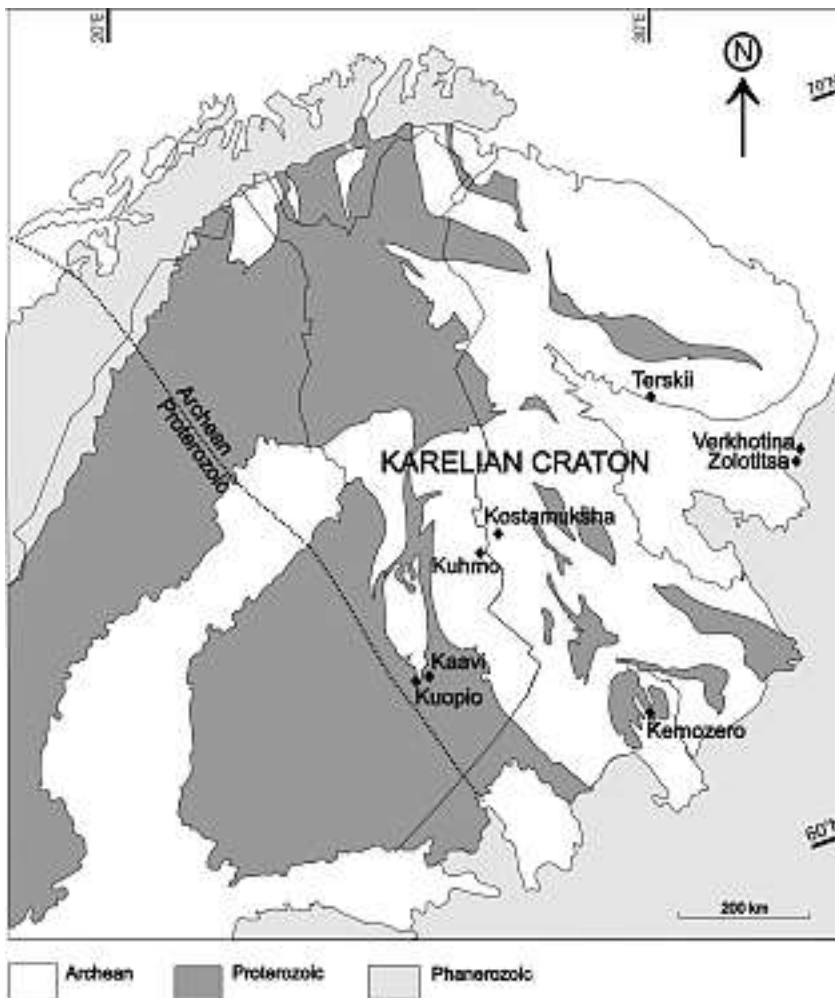


Fig. 1. Generalized geological map of Fennoscandia. The Archean/Proterozoic boundary marks the subsurface extent of the Archean craton as determined by Nd isotopes. The black diamonds represent diamond-bearing kimberlites and lamproites.

(Lehtonen et al., 2004): 1. An upper zone, shallower than 110 km, distinguished by Ca-saturated but Ti-, Y- and Zr-depleted pyropes. The rare xenoliths originating from this layer are garnet-spinel harzburgites, containing secondary Cpx. 2. A garnet peridotite zone occurs at 110 to 180 km depth, and ranges in bulk composition from harzburgite to lherzolite to wehrlite. 3. A deep, more fertile zone, from 180 to 240 km, from where the bulk of the garnet facies peridotite xenoliths were derived. Mantle eclogite xenoliths originate also from this deepest layer, some of them being highly diamondiferous (Peltonen et al., 2002). The stabilization ages of these distinct mantle layers are still to be resolved but at least the upper and the middle layers are believed to be Archean, with a similar age to that of the overlying crust (Pearson, 1999). The lowermost layer may represent Archean lithospheric mantle that has been considerably re-fertilized by melt metasomatism (Lehtonen et al., 2004). Alternatively it is possible that this section of the mantle has been tectonically emplaced during the Svecofennian collision event at 1.88 Ga (Peltonen et al., 1999). Re-Os isotope measurements on mantle xenoliths will eventually provide direct evidence on the stabilization ages of the different mantle horizons (Peltonen & Brüggemann, submitted).

The aim of this study was to obtain additional information on the composition, origin and evolutionary history of the stratified lithospheric mantle underlying Kaavi-Kuopio by studying major, trace, and rare-earth element contents of peridotitic garnet xenocrysts from five kimberlite pipes. Garnet xenocrysts do not contain as much information as mantle xenoliths because coexisting minerals are not available, but they are far more abundant in kimberlites and in principle provide a statistically robust sample of the underlying mantle (Schulze, 1995). The trace element contents of garnets and the shapes of their rare-earth element (REE) patterns normalized to C1-chondrite composition, record a diverse range of geochemical behavior controlled by pressure, temperature and composition of their host rock, which themselves are related to the origin, provenance and thermal history of the mantle (e.g. Griffin et al., 1999a,

1999b; Canil et al., 2003). Garnet is a sensitive petrogenetic indicator, since it has very low D values for the light REE and increasingly larger D's for the heavy REE (Green, 1980), and provides information about depletion and metasomatic events prevalent in the lithospheric mantle prior to, or contemporaneous with, the kimberlite magmatism.

## 2. Samples

Samples were selected from five Kaavi-Kuopio Province kimberlites, Lahtojoki, Kylmälahti, Kärenpää, Niilonsuo and Ryönä (Table 1). In the case of Lahtojoki and Kylmälahti kimberlites xenocryst grains (0.25–2.0 mm) were liberated by lightly crushing the kimberlite material followed by heavy medium separation and hand picking. The hard magmatic Niilonsuo kimberlite was processed in a similar way but first fragmented electro-dynamically at Forschungszentrum Karlsruhe GmbH. The Kärenpää and Ryönä samples were heavy mineral concentrates handed over to the Geological Survey of Finland (GTK) by Malmikaivos Oy (Tyni, 1997).

Thousands of garnet xenocrysts were recovered from the kimberlite concentrates out of which c. 1300 were selected for analysis (Table 1). In this study an unsorted population of xenocrysts has been used in order to get unbiased information on the garnets present within the kimberlites. Except for the garnet-poor Niilonsuo kimberlite, the number of analyzed garnets per kimberlite does not represent (even though loosely correlates with) the total number of garnets within the sample.

## 3. Analytical techniques

Garnet major element compositions were determined by a Cameca Camebax SX50 electron microprobe (EMP) at GTK, applying an acceleration voltage of 25 kV, probe current of 48 nA and beam diameter of 1 µm. Selected garnet xenocrysts were analyzed for trace elements by LA-ICP-MS at the University of Cape Town using the methodology and equipment described in Grégoire et al. (2003). Typical theoretical detection limits are in the range of 10–20 ppb

**Table 1.** Description of kimberlite samples and the number of garnets selected for major and trace element analysis.

Kimberlite	Pipe number	Location	Size	Sample type	Sample size	Garnet majors	Garnet traces*	Garnet REE
Lahtojoki	7	Kaavi	2 ha	weathered kimberlite material	~4 kg	614	192	73
Kylmälahti	17	Kuopio	2 ha	drill core	~1 kg	188	102	57
Kärenpää	5	Kaavi	700 x 30 m	concentrate	~100 g	95	12	
Niilonsuo	2	Kaavi	300 x 50 m	kimberlite boulders	~2 kg	18	9	
Ryönä	10	Kuopio	2 ha	concentrate	~100 g	392	186	
Total						1307	501	130

\*) Ni,  $\pm$ Y,  $\pm$ Zr,  $\pm$ Ga,  $\pm$ Sc

for REE, Zr and Y, and 2 ppm for Ti and Ni. Trace Ni data by EMP were obtained on pyrope grains employing 500 nA probe current, 600 s counting times on peak plus background positions and were reduced by the CSIRO TRACE program for the SX50 (Robinson & Graham, 1992). Cross-checking of the trace methods shows that Ni analyses in pyrope by EMP can achieve similar precision to those of LA ICP-MS down to the level of ca. 10 ppm.

The garnets were classified based on their major element composition into harzburgitic, lherzolitic, wehrlitic, megacrystal, eclogitic and crustal varieties according to Schulze (2003). In addition, the term “CCGE” which stands for “chromite-clinopyroxene-garnet equilibrium” was adopted from Kopylova et al. (2000) for distinctive Ca-saturated garnets, which in this study have low Ti, Y and Zr. For equilibration temperatures the Ni thermometer (Griffin et al., 1989a) was applied using the calibration of Ryan et al. (1996).

## 4. Review of previous results

Major part of the following results of garnet geochemistry and Ni thermometry from Kaavi-Kuopio kimberlites has been discussed already in Lehtonen et al. (2004). However, this study also contains major and trace element data on garnets from Ryönä kimberlite (Table 1), which was not included in the previous study. Selected major and trace element analyses for pyrope xenocrysts are presented in Table 2. The entire analytical database is available as an Open file at the Geological Survey of Finland (Lehtonen et al.,

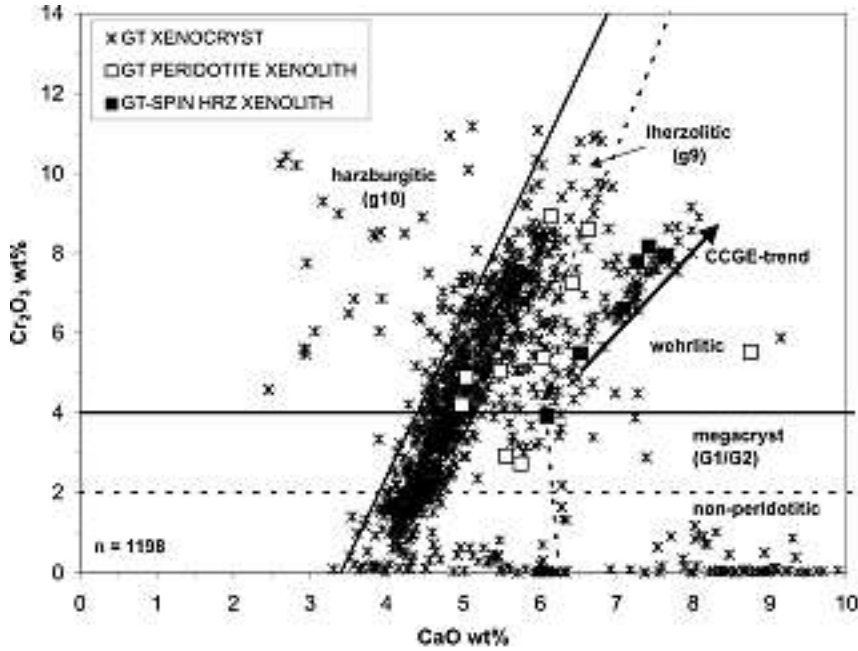
2005) or can be requested from the author by e-mail. Major and trace element analyses from garnets in the Kaavi-Kuopio mantle xenoliths have been published in Peltonen et al. (1999).

### 4.1. Garnet major element geochemistry

CaO and Cr<sub>2</sub>O<sub>3</sub> contents of garnets from Kaavi-Kuopio peridotite xenoliths and garnet xenocrysts are shown in Figure 2 and the classification of xenocrysts based on Schulze (2003) is presented in Figure 3. It is evident that lherzolitic garnet predominates over other garnet varieties. Moreover, a well-developed pyrope trend (CCGE) exists similar to that described by Kopylova et al. (1999; 2000) and Carbno & Canil (2002) from the Slave craton (Fig. 2). Orange relatively Cr-poor but Ti-rich pyropes of megacryst composition are also common among the xenocrysts. A few grains in the lower right corner of the CaO-Cr<sub>2</sub>O<sub>3</sub> diagram, at high levels of Ca and low levels of Cr, fall into the “eclogitic” category (Schulze, 2003). None of the garnets from xenoliths and only a minor portion of the garnet xenocrysts are classified as subcalcic harzburgitic grains.

### 4.2. Garnet thermometry and trace element geochemistry

The T<sub>Ni</sub> histogram in Figure 4 for Kaavi-Kuopio garnet xenocrysts shows bimodal distribution including a strong low temperature peak at 700 to 850°C consisting dominantly of CCGE pyropes and a stronger



sampling peak at 1000 to 1150°C consisting of lherzolitic, harzburgitic and megacryst varieties. CCGE pyropes do not occur at higher temperatures than 850°C. Based on the Y contents of garnets, 1150°C represents another break in the lithosphere, separating mantle that contains strongly depleted pyropes from more enriched mantle, as seen in Figure 5 where  $T_{Ni}$  temperatures have been extrapolated to the local geotherm (Kukkonen and Peltonen, 1999; Kukkonen et al., 2003). The “Y edge” (terminology after Griffin & Ryan, 1995) does not mark the lower boundary of the lithosphere, as all xenoliths from >1150°C are coarse granular peridotites typical of subcontinental lithospheric mantle (Peltonen et al., 1999). Figure 5 shows that the main horizon of sampling at 1000 to 1150°C corresponds to the mantle section from 140 to 175 km.

The two breaks, 850 and 1150°C, in the mantle stratigraphy show up as well using the  $TiO_2$  contents and Mg# of garnets (Fig. 6). Variations in the pyrope  $TiO_2$  contents as a function of temperature closely follow the same pattern as the pyrope Y contents, since both of these elements reflect the degree of depletion or enrichment within the mantle (e.g. Griffin & Ryan, 1995). Mg# is a substantially different parameter of garnet composition than Ti and Y. Mg# of

Fig. 2.  $Cr_2O_3$  vs. CaO of Kaavi-Kuopio kimberlite-derived garnets. The xenocryst data are representative of the entire mantle garnet population of the pipes. Crustal garnets are excluded from this diagram using the classification by Schulze (2003). The harzburgite, lherzolite and non-peridotite fields are redrawn after Gurney (1984) and the wehrlite field is separated according to Sobolev et al. (1973). Arrow pointing NE marks the “CCGE” garnet trend, i.e. chromite-clinopyroxene-garnet equilibrium, recognized in spinel-garnet peridotites from the Jericho kimberlite (Kopylova et al., 2000).

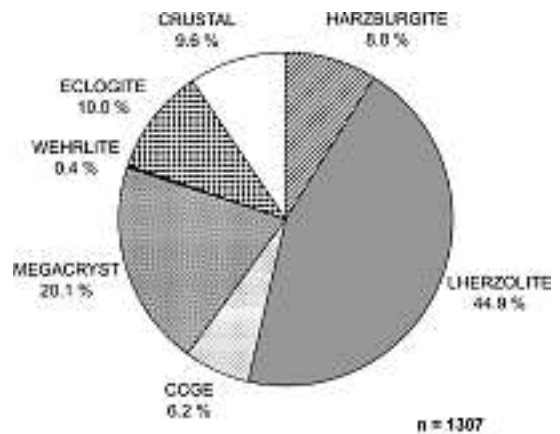


Fig. 3. Classification of garnet xenocrysts recovered from heavy mineral concentrates according to the scheme of Schulze (2003). Term “CCGE” adopted from Kopylova et al. (2000) for distinct garnets (discussed in text); using the Schulze classification these garnets would be labelled as lherzolitic varieties.

**Table 2.** Representative\*) electron microprobe and LA-ICP-MS analyses of garnet xenocrysts from Finnish kimberlites.

Sample ID	Schulze 03	Comment	EPMA analyses										Total wt%
			SiO <sub>2</sub> wt%	TiO <sub>2</sub> wt%	Al <sub>2</sub> O <sub>3</sub> wt%	Cr <sub>2</sub> O <sub>3</sub> wt%	FeO wt%	MnO wt%	MgO wt%	NiO wt%	CaO wt%	Na <sub>2</sub> O wt%	
4682.02	Lherzolite	CCGE	39.61	0.05	20.21	5.01	8.74	0.48	18.35	0.00	6.38	0.00	98.92
10657.02	Lherzolite	CCGE	40.17	0.00	17.68	7.55	8.25	0.53	17.16	0.00	7.44	0.00	98.83
4398.96	Lherzolite	CCGE	40.83	0.00	17.01	8.62	7.74	0.56	17.60	0.00	7.67	n.a.	100.08
10000.02	Lherzolite	CCGE	40.16	0.01	17.90	7.55	8.20	0.51	17.60	0.00	7.43	0.01	99.40
#9	Lherzolite	Simpl. type	40.18	0.04	17.83	7.39	7.85	0.55	19.07	0.00	5.54	n.a.	98.44
#31	Harzburgite	Simpl. type	40.94	0.02	18.60	6.58	8.34	0.61	19.65	0.00	4.72	n.a.	99.47
8101.96	Lherzolite	Simpl. type	40.65	0.24	14.50	10.87	6.62	0.39	19.34	0.01	6.70	n.a.	99.48
8103.96	Lherzolite	Simpl. type	40.62	0.27	14.41	10.94	6.58	0.41	19.24	0.02	6.74	n.a.	99.35
4403.96	Harzburgite	Sinusoidal	42.19	0.03	19.35	6.05	6.44	0.36	23.19	0.01	3.06	n.a.	100.69
#43	Harzburgite	Sinusoidal	41.00	0.28	17.24	8.08	6.22	0.32	20.81	0.01	5.18	n.a.	99.16
15947.01	Harzburgite	Sinusoidal	41.05	0.11	16.81	8.49	6.31	0.32	21.26	0.01	4.24	n.a.	98.68
15946.01	Harzburgite	Sinusoidal	41.34	0.31	18.08	6.59	6.49	0.29	21.04	0.01	4.83	n.a.	99.00
15971.01	Harzburgite	Sinusoidal	40.89	0.07	15.90	10.21	6.31	0.36	22.35	0.02	2.82	n.a.	98.95
18078.01	Lherzolite	Sinusoidal	41.16	0.34	17.46	7.57	7.03	0.41	20.26	0.01	5.56	n.a.	99.82
18092.01	Lherzolite	Sinusoidal	40.87	0.25	16.93	8.39	6.90	0.38	19.81	0.01	6.05	n.a.	99.58
13374.95	Lherzolite	Sinusoidal	41.05	0.36	16.64	8.56	6.65	0.40	20.04	0.01	6.05	n.a.	99.91
4686.02	Lherzolite	Sinusoidal	40.18	0.03	18.57	5.90	6.80	0.26	20.95	0.02	5.78	0.01	98.65
15995.01	Wehrlite	N-type	41.03	0.58	19.20	4.49	9.93	0.51	17.29	0.01	7.28	n.a.	100.33
#106	Lherzolite	N-type	40.04	0.53	17.31	6.89	8.98	0.53	17.58	0.01	6.85	n.a.	98.76
#94	Lherzolite	N-type	39.99	0.91	15.99	7.71	9.27	0.42	17.64	0.01	6.87	n.a.	98.82
15924.01	Lherzolite	N-type	40.14	0.88	17.62	5.70	9.35	0.42	17.84	0.01	6.37	n.a.	98.38
10660.02	Lherzolite	N-type	40.21	0.90	16.82	6.24	9.75	0.42	18.04	0.01	6.12	0.11	98.69
4674.02	Lherzolite	N-type	39.58	0.15	20.11	4.55	8.56	0.42	19.91	0.01	5.20	0.05	98.59
10635.02	Lherzolite	N-type	40.69	0.54	19.37	4.08	8.52	0.40	19.39	0.01	5.55	0.09	98.69
13358.95	Lherzolite	N-type	41.13	0.55	19.75	4.35	7.05	0.41	20.80	0.01	4.83	n.a.	99.06
4692.02	Lherzolite	N-type	39.72	0.63	19.71	4.18	8.48	0.41	19.63	0.01	5.40	0.07	98.33
4611.02	Lherzolite	N-type	40.37	0.86	18.67	5.49	7.29	0.38	20.46	0.00	5.32	0.11	98.99
#11	Lherzolite	N-type	40.36	0.61	16.74	7.86	8.20	0.48	19.04	0.00	5.97	n.a.	99.27
8108.96	Lherzolite	N-type	42.41	0.47	19.92	3.73	6.71	0.31	22.14	0.02	4.72	n.a.	100.59
18147.01	Lherzolite	N-type	41.44	0.54	19.45	4.01	7.58	0.28	21.20	0.01	4.80	n.a.	99.42
18155.01	Lherzolite	N-type	41.55	0.56	18.95	5.05	7.06	0.30	21.00	0.01	5.25	n.a.	99.76
18077.01	Lherzolite	N-type	41.43	0.56	17.25	6.96	6.73	0.28	20.91	0.01	5.57	n.a.	99.75
8109.96	Lherzolite	N-type	41.27	0.60	19.25	4.07	7.73	0.37	20.89	0.02	4.94	n.a.	99.30
10634.02	Lherzolite	N-type	40.33	0.89	17.28	6.28	8.45	0.44	19.02	0.01	6.04	0.09	98.86
#17	Lherzolite	N-type	41.68	0.41	20.88	2.39	7.14	0.30	21.69	0.01	4.63	n.a.	99.19
4703.02	Lherzolite	N-type	40.93	0.49	21.04	2.40	8.23	0.33	21.58	0.02	4.40	0.06	99.56
4669.02	Lherzolite	N-type	41.06	0.49	21.11	2.01	8.18	0.29	21.19	0.01	4.70	0.05	99.14
#22	Lherzolite	N-type	40.89	0.03	19.54	5.09	8.49	0.55	19.11	0.00	5.72	n.a.	99.52
13362.95	Megacryst	N-type	41.46	0.52	21.11	2.08	7.71	0.32	21.13	0.02	4.41	n.a.	98.91
4655.02	Megacryst	N-type	40.50	0.64	21.05	2.16	8.03	0.28	21.31	0.01	4.76	0.04	98.88
18160.01	Megacryst	N-type	41.28	0.65	20.57	2.51	8.33	0.29	20.90	0.01	4.85	n.a.	99.41
4672.02	Megacryst	N-type	40.23	0.77	20.23	2.91	8.50	0.34	20.67	0.01	5.00	0.06	98.79
8114.96	Megacryst	N-type	41.30	0.64	20.74	1.48	9.07	0.37	20.76	0.02	4.23	n.a.	98.79

\*) The entire analytical database is available as the Geological Survey of Finland Open file report M 41.2/2005/1 (Lehtonen et al., 2005)

Schulze 03 = Schulze (2003); RGP96 = Ryan et al. (1996)

n.a. = not analyzed

n.d. = not detected

LA-ICP-MS analyses																TNi (Co) RGP96
Sc ppm	Ni ppm	Ga ppm	Y ppm	Zr ppm	La ppm	Ce ppm	Nd ppm	Sm ppm	Eu ppm	Gd ppm	Dy ppm	Er ppm	Yb ppm	Lu ppm		
135	12	2.2	2.8	3.8	0.08	0.13	0.53	0.18	0.08	0.18	0.28	0.51	0.62	0.25	688	
208	20	2.8	0.2	0.8	0.09	0.16	0.13	0.17	0.08	0.09	0.11	n.d.	0.35	0.08	795	
284	23	2.5	0.5	2.4	0.13	1.01	1.06	0.17	0.03	0.18	0.16	0.01	0.34	0.14	826	
197	19	2.5	0.3	1.2	0.08	0.28	0.33	0.15	0.04	0.16	0.05	0.08	0.36	0.14	777	
220	21	2.4	17.3	44.6	0.03	0.85	5.63	3.48	1.35	4.49	3.70	1.39	1.32	0.28	803	
175	22	3.4	6.6	40.0	0.02	0.80	4.07	3.03	1.18	4.11	2.09	0.37	0.09	0.08	814	
128	71	9.0	19.9	41.2	0.22	1.21	6.39	5.41	1.90	7.19	4.76	1.28	1.02	0.23	1154	
131	71	8.9	20.2	43.9	0.20	1.07	7.23	5.75	2.11	6.73	4.77	1.76	0.74	0.18	1156	
113	50	3.1	1.1	3.9	0.12	0.36	2.95	0.82	0.19	0.57	0.17	0.18	0.11	0.11	1034	
119	62	11.3	3.2	15.8	0.12	0.46	1.53	0.63	0.20	0.70	0.57	0.37	0.70	0.15	1106	
171	65	5.1	3.3	5.7	0.07	0.78	2.94	1.06	0.27	0.98	0.51	0.42	0.48	0.07	1122	
130	66	5.5	3.4	21.4	0.08	0.29	1.07	0.92	0.27	1.07	0.89	0.54	0.70	0.06	1124	
158	67	2.9	1.0	18.8	0.08	0.54	3.06	2.04	0.46	1.39	0.32	0.06	0.24	0.07	1134	
147	55	3.8	4.4	38.0	0.08	0.37	1.44	1.07	0.32	1.67	1.17	0.38	0.47	0.14	1061	
140	53	3.4	1.0	13.3	0.12	n.d.	1.61	0.73	0.08	0.30	0.12	0.11	0.47	0.05	1047	
141	77	4.9	1.9	18.7	0.08	0.41	1.53	0.94	0.19	0.86	0.34	0.23	0.35	0.13	1185	
128	100	5.3	1.3	1.2	0.14	0.71	1.21	0.46	0.13	0.11	0.09	0.18	0.53	0.12	1297	
138	44	13.9	25.2	64.3	0.06	0.39	1.22	1.09	0.67	2.57	4.71	3.07	3.08	0.44	993	
141	46	9.1	22.5	63.9	0.10	0.43	1.46	1.03	0.56	2.95	4.17	2.36	2.18	0.35	1006	
118	57	13.9	17.5	50.2	0.12	0.35	1.05	0.78	0.40	2.01	2.97	2.24	1.95	0.30	1071	
123	59	14.9	17.0	46.2	0.12	0.52	1.41	0.87	0.46	1.64	3.07	2.27	2.36	0.41	1084	
115	64	15.2	16.8	49.0	0.11	0.33	0.93	0.74	0.46	2.20	3.02	1.83	1.74	0.25	1112	
124	34	4.6	13.1	46.5	0.06	0.45	1.84	1.32	0.53	2.02	2.25	1.39	1.27	0.24	918	
96	46	9.7	15.6	42.3	0.04	0.23	0.98	0.57	0.36	1.39	2.98	1.75	1.54	0.35	1004	
90	52	7.0	11.5	28.3	0.06	0.22	0.74	0.62	0.26	1.23	1.84	1.16	1.68	0.23	1041	
86	38	8.2	14.7	34.2	0.05	0.21	0.70	0.45	0.32	1.43	2.60	1.70	1.55	0.26	947	
110	63	9.2	14.2	44.6	0.04	0.29	0.90	0.79	0.43	1.58	2.55	1.52	1.77	0.24	1109	
123	40	5.7	14.0	43.4	0.04	0.33	1.60	1.08	0.46	1.83	2.54	1.21	1.11	0.19	964	
94	112	7.8	10.9	28.6	0.05	0.30	1.38	0.66	0.27	1.38	1.90	1.02	1.43	0.28	1355	
113	84	7.9	13.6	35.1	0.09	0.24	1.07	0.65	0.29	1.19	2.50	1.30	1.39	0.26	1222	
113	79	8.6	12.8	43.3	0.09	0.30	1.28	0.87	0.26	1.47	2.27	1.29	0.97	0.20	1196	
135	118	6.8	10.3	41.0	0.07	0.45	2.15	0.98	0.33	1.74	1.70	1.24	0.94	0.19	1383	
102	72	9.2	13.4	39.3	0.03	0.24	1.02	0.71	0.35	1.45	2.09	1.36	1.87	0.31	1160	
101	71	14.2	15.0	44.3	0.05	0.30	0.93	0.80	0.52	1.65	2.83	1.79	1.95	0.32	1155	
83	77	6.7	11.0	31.8	0.05	0.32	0.75	0.56	0.31	1.03	1.86	1.50	1.50	0.24	1188	
84	83	7.6	12.8	27.1	0.04	0.24	0.70	0.45	0.40	0.85	1.87	1.59	1.68	0.35	1216	
94	86	8.3	12.4	33.7	0.06	0.30	1.13	0.66	0.39	1.41	1.84	1.52	1.56	0.35	1234	
92	77	7.3	9.2	28.4	0.15	0.54	0.96	0.51	0.30	0.91	1.96	1.19	1.40	0.22	1185	
73	86	9.6	13.4	25.9	0.04	0.25	0.66	0.55	0.29	1.32	1.95	1.69	1.77	0.29	1233	
98	80	8.3	13.6	37.3	0.11	0.37	0.80	0.74	0.42	1.27	2.03	1.52	2.10	0.32	1202	
94	77	10.4	14.3	40.1	0.04	0.22	0.90	0.63	0.33	1.02	2.28	1.45	1.91	0.32	1187	
111	63	9.5	14.7	42.5	0.02	0.25	0.91	0.55	0.31	1.25	2.32	1.94	2.03	0.28	1108	
96	71	9.9	16.2	38.8	0.04	0.20	0.83	0.50	0.32	1.67	2.98	2.19	2.40	0.44	1155	

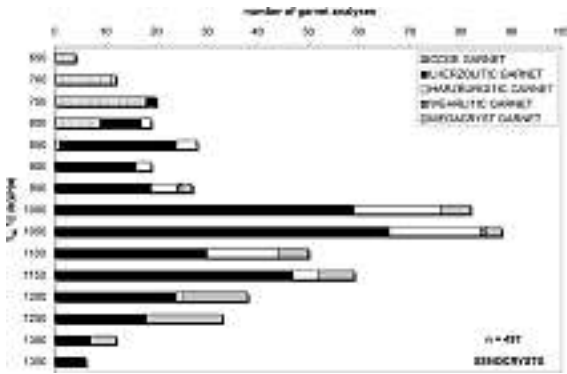


Fig. 4. Distribution of  $T_{Ni}$  for Kaavi-Kuopio pyrope xenocrysts using the calibration of Ryan et al. (1996). Ti-rich megacryst composition garnets are included for illustrative purposes. Megacryst garnets with  $Cr_2O_3 > 1.5$  wt% and  $MgO > 18$  wt% are shown as they reach the same contents of these elements as do lherzolitic pyropes, implying equilibration with olivine similar to that in the lherzolites.

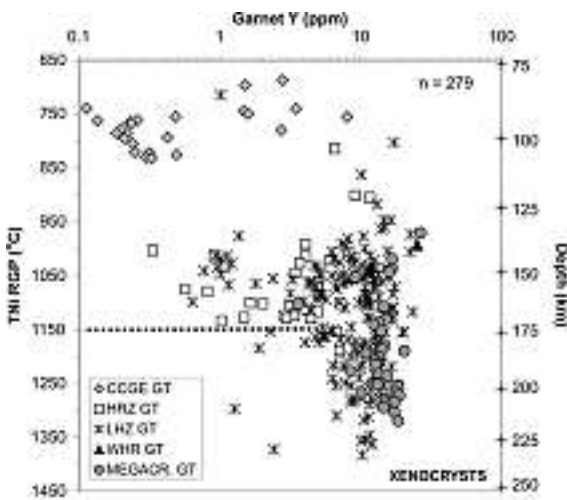


Fig. 5. Y contents of pyropes vs.  $T_{Ni}$  (Ryan et al., 1996) show an edge at about 1150°C (modified from Lehtonen et al., 2004). Depths marked on the right vertical axis of the diagram are calculated by extrapolating the  $T_{Ni}$  temperatures of pyropes to the local geotherm determined by Kukkonen et al. (2003). Cr-rich ( $Cr_2O_3 > 1.5$  wt%) megacryst composition grains are included in the diagrams, see Fig. Cap. 4.

garnet reflects bulk composition but it is also strongly controlled by the temperature dependent Mg-Fe exchange with olivine, Opx, Cpx and Mg-chromite

(Stachel et al., 2003). Moreover, Ca has a significant crystal chemical effect on the Mg-Fe partitioning between garnet and olivine (Stachel et al., 2003; O'Neill & Wood, 1979). The lower temperature boundary at c. 850°C corresponds to the break in  $TiO_2$  at approximately 110 km depth and separates extremely low Ti content CCGE pyropes with Mg# around 0.80 from a lherzolitic and harzburgitic (and wehrlitic) horizon exhibiting a wide range in both parameters. The second boundary roughly at 1150°C or ca. 175 km is the limit below which only a very few  $TiO_2$ -depleted pyropes occur and pyrope Mg# values are less variable. Harzburgitic garnets with depleted Y and Ti contents exist only at temperatures below 1150°C; the rare depleted grains from higher temperatures are all lherzolitic varieties (Figs. 5 and 6a). In the middle mantle layer (110–175 km) there exists a distinctive group of garnets with low Mg# (0.76–0.78) that is absent in the other two mantle horizons. These garnets are classified as lherzolitic and wehrlitic varieties according to Schulze (2003) but probably represent melt-metasomatic garnets based on their high Fe and Ti contents. In Figure 6a they plot among the most Ti-rich garnets, by having  $TiO_2$  in the range of 0.5–1.0 wt%. Y contents of these low Mg# garnets are also elevated ( $> 10$  ppm): in Figure 5 they plot with the bulk of the middle temperature garnets. According to the Zr-Y classification by Griffin & Ryan (1995; Fig. 7) the Kaavi-Kuopio garnet xenocrysts from the middle and the lower mantle layer (lherzolitic, wehrlitic and megacryst varieties) bear evidence of melt metasomatism, which appears to have been a prevalent process in the deeper levels of the upper mantle prior to, or contemporaneous with kimberlite magmatism. A phlogopite (hydrous) metasomatic trend seems to be absent in all xenocrysts (Fig. 7).

## 5. Results

Figure 8 shows C1-chondrite-normalized (McDonough & Sun, 1995) rare-earth element (REE) profiles of garnets from the Kaavi-Kuopio Province peridotite xenoliths (Fig. 8a; Peltonen et al., 1999) and selected garnet xenocrysts (Figs. 8b–8g). Based on



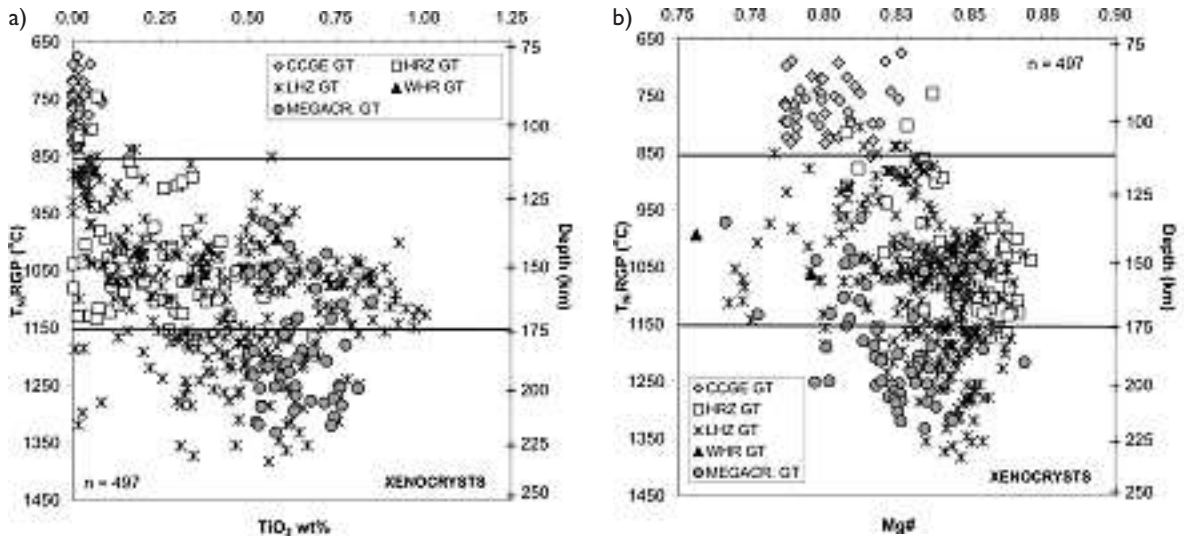


Fig. 6.  $TiO_2$  a) and  $Mg\#$  b) vs.  $T_{Ni}$  (Ryan et al., 1996) and depth for the Kaavi-Kuopio xenocryst pyropes showing three distinct layers of the underlying mantle. Depths are calculated as in Fig. 5. Cr-rich ( $Cr_2O_3 > 1.5$  wt%) megacryst composition grains are included in the diagrams, see Fig. 4.

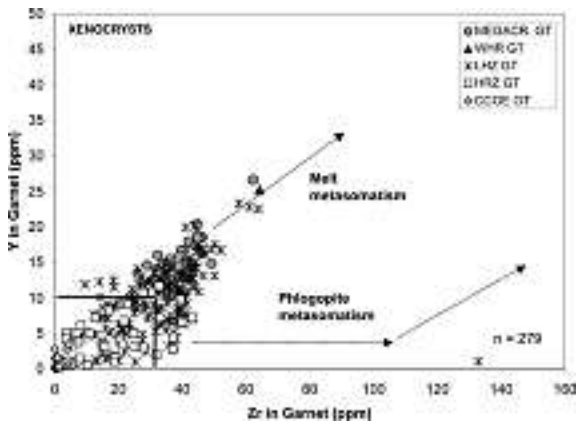


Fig. 7. Y vs. Zr for the Kaavi-Kuopio pyrope xenocrysts (from Lehtonen et al., 2004). Melt and phlogopite metasomatism trends are drawn after Griffin and Ryan (1999b). Solid black line defines the depleted field.

major and trace element compositions and Ni thermometry results described in section 4, the garnet xenocrysts can be classified into six classes, as listed in Table 3. These are discussed further below.

**5.1. Rare-earth element contents of garnets in peridotite xenoliths**

The  $REE_N$  patterns of garnets in the garnet facies peridotite xenoliths (Fig. 8a) are very similar regardless of

their host rock type (lherzolite, harzburgite or wehr-lite defined by modal petrography), showing strong LREE depletion relative to MREE and HREE with steady enrichment from  $Sm_N$  to  $Yb_N$ , typical of Ca-saturated mantle garnets (e.g. Shimizu, 1975). This type of garnet  $REE_N$  patterns are herein termed “N-type”. Garnets from garnet-spinel facies harzburgite xenoliths have ultra-depleted  $REE_N$  profiles, particularly in terms of MREE and HREE. Garnet analyzed from a phlogopite- and Cpx-bearing garnet-spinel symplectite in L14 xenolith has a convex-upward  $REE_N$  pattern that shows strong MREE (Nd to Eu) enrichment followed by a decrease towards HREE. The symplectites have been taken to represent decomposed primary garnet (Peltonen et al., 1999).

**5.2. Rare-earth element contents of peridotitic garnet xenocrysts**

The  $REE_N$  profiles of all garnet xenocrysts classified as megacrysts (Table 3, Class 6; Fig. 8g) and most of the xenocrysts classified as intermediate temperature (Class 4; Fig. 8e) to high temperature (Class 5; Fig. 8f) lherzolitic pyropes are N-type, similar to those from the garnet facies peridotite xenoliths described above. A subset of the Ti- and Y ± Zr poor

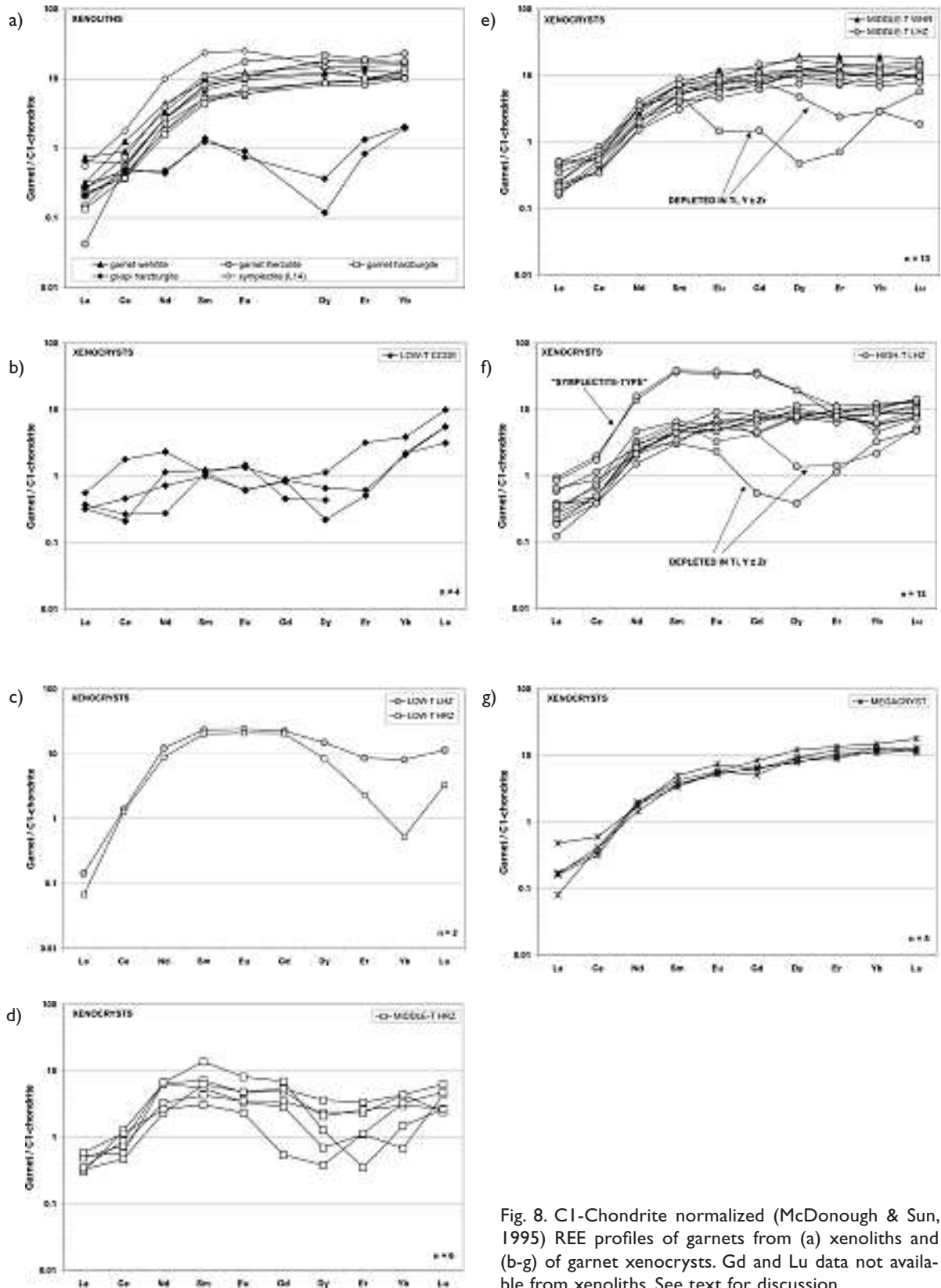


Fig. 8. CI-Chondrite normalized (McDonough & Sun, 1995) REE profiles of garnets from (a) xenoliths and (b-g) of garnet xenocrysts. Gd and Lu data not available from xenoliths. See text for discussion.

**Table 3.** Garnet xenocryst classification based on major and trace element geochemistry and Ni thermometry.

Class	Classification Schulze (2003)	TNi (oC) garnet Ryan et al. (1996)	Mantle layer (km)	Figure	REE profile normalized to C1-chondrite (McDonough & Sun, 1995)
1	CCGE*	< 850	< 110	8B	ultra-depleted
2	LHZ, HRZ	< 850	< 110	8C	convex upward (i.e. symplectite-type)
3	HRZ	850–1150	110–175	8D	sinusoidal
4	LHZ, WHR	850–1150	110–175	8E	N-type, rare sinusoidal
5	LHZ	> 1150	> 175	8F	N-type, very rare sinusoidal or symplectite-type
6	MEGACR.	mostly > 1150	mostly > 175	8G	N-type

\*) Classification after Kopylova et al. (2000) for distinctive Ca-saturated and Ti-, Y and Zr-depleted pyropes. Classified as lherzolitic pyropes according to Schulze (2003).

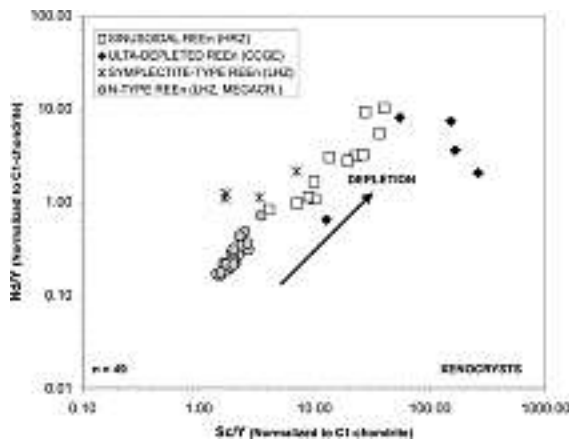


Fig. 9. Sc/Y (N) vs. Nd/Y (N) for garnet xenocrysts. (N = normalized to C1-chondrite composition after McDonough & Sun, 1995).

(TiO<sub>2</sub> < 0.4 wt%; Y ± Zr < 10 ppm) lherzolitic and nearly all of the intermediate temperature harzburgitic (Class 3; Fig. 8d) grains have sinusoidal REE<sub>N</sub> patterns, diagnostic for subcalcic harzburgitic garnets (e.g. Shimizu, 1975). The positive slope from La<sub>N</sub> to Nd<sub>N</sub> is due to a strong increase in compatibility in the garnet structure with decreasing ionic radius of the LREE from La to Nd (e.g. Stachel et al., 1998). The sinusoidal REE<sub>N</sub> profile is characterized by enrichment in Sm over Dy, and LREE enrichment, as measured, for instance by (Nd/Y)<sub>N</sub> greater than unity (Fig. 9). The (Nd/Y)<sub>N</sub>, in fact, distinguishes garnets with sinusoidal REE<sub>N</sub> patterns and (Nd/Y)<sub>N</sub> > 1, from those with LREE depleted N-type patterns and (Nd/Y)<sub>N</sub> < 1 (Pearson et al., 1998). The (Sc/Y)<sub>N</sub> ratio of garnets (Fig. 9) provides a measure of the depletion of HREE, since Sc is preferentially accommodat-

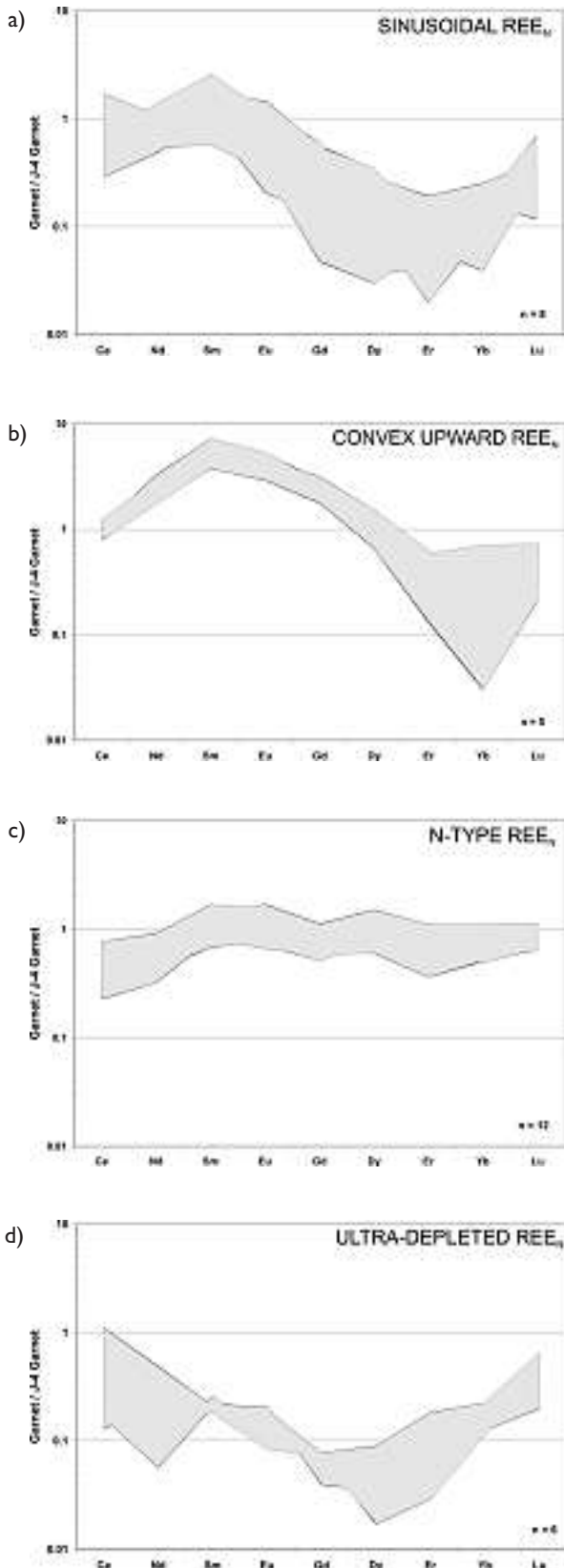
ed into garnet during depletion. Values of (Sc/Y)<sub>N</sub> > 1 are characteristic of depleted compositions, whereas (Sc/Y)<sub>N</sub> ~ 1 are obtained from undepleted garnet varieties (Pearson et al., 1998).

The ultra-depleted REE<sub>N</sub> profiles of the low temperature CCGE garnet xenocrysts (Class 1; Fig. 8b) coincide with those from garnets in the garnet-spinel harzburgite xenoliths (Fig. 8a). These REE<sub>N</sub> profiles show a distinct positive slope in HREE from Er/Dy to Lu. This slope has been interpreted to represent the memory of a previous melt depletion event (Stachel et al., 1998). In Figure 9 CCGE garnets are clearly distinct from the other garnet varieties with high (Sc/Y)<sub>N</sub> and (Nd/Y)<sub>N</sub> indicating extreme depletion.

The rare low temperature garnet xenocrysts other than CCGE's, i.e. lherzolitic and harzburgitic grains (Class 2; Fig. 8c), have similar convex-upward REE<sub>N</sub> patterns to garnet analyzed from L14 xenolith (Fig. 8a). Garnet xenocrysts with this type of REE<sub>N</sub> patterns also form a minor portion of the high temperature lherzolitic grains (Class 5, Fig. 8f) but are absent among the intermediate temperature xenocrysts. In Figure 9 these "symplectite-type" garnets partially overlap with the sinusoidal varieties by having (Nd/Y)<sub>N</sub> ratios within the range 1–3 but stand out from them by having lower (Sc/Y)<sub>N</sub> ratios, i.e. closer to unity.

## 6. Discussion

Figure 10 presents the REE profiles of garnets from the peridotite xenoliths and garnet xenocrysts normalized to a garnet from a well-equilibrated high-temperature sheared lherzolite xenolith with primi-



tive, undepleted mantle composition (J-4 from Jagersfontein; Table 1 in Stachel et al., 1998). Normalization to a primitive garnet instead of C1-chondrite has the advantage that the resulting REE patterns are not dominated by crystal chemical effects, such as the strong increase in compatibility with decreasing ionic radius from LREE to HREE. From the garnet REE contents the following evolutionary history can be suggested for the lithospheric mantle underlying Kaavi-Kuopio.

### 6.1. Stage 1: Sinusoidal garnet formation

The sinusoidal REE<sub>N</sub> profiles (Fig. 10a) of the subcalcic harzburgitic (Class 3) and the rare Ti-poor lherzolitic (Classes 4 and 5) garnet xenocrysts indicate that the primitive mantle experienced an extensive komatiite melt extraction event similar to that observed elsewhere, resulting in extreme LREE and HREE depletion, the first step in the formation of cratonic peridotites (e.g. Shimizu & Richardson, 1987; Nixon et al., 1987; Stachel et al., 1998). Subsequently the lithosphere was most likely composed of highly depleted garnet harzburgite and Ti-poor lherzolite, the residues of this melt extraction process. Sinusoidal REE<sub>N</sub> patterns were developed as a result of fluid metasomatism involving introduction of (repeated) pulses of a fractionated fluid/melt with low HREE and variable LREE/MREE into the depleted lithosphere (Stachel et al., 2004). With respect to their Y and Zr contents, the subcalcic harzburgitic garnets plot in the compositional field of depleted garnets (Fig. 7), underlining the highly fractionated

Fig. 10. The four principal types of Kaavi-Kuopio garnets according to their REE patterns normalized to garnet from a well-equilibrated garnet lherzolite xenolith with primitive mantle composition (J-4 from Jagersfontein, Stachel et al., 1998). a) sinusoidal subcalcic harzburgitic and rare sinusoidal Ti-poor lherzolitic garnet xenocrysts b) convex upward garnet xenocrysts and a garnet from a symplectite in L14 xenolith c) garnets from garnet peridotite xenoliths and N-type lherzolitic and megacryst garnet xenocrysts, and d) ultra-depleted CCGE garnet xenocrysts and garnets from garnet-spinel harzburgite xenoliths. See text for discussion.

character the fluid/melt must have had. The sinusoidal REE pattern was previously thought to arise from disequilibrium effects, causing the larger LREE cations to diffuse faster than the smaller HREE in garnet structure (Hoal et al., 1994), but experiments do not confirm this process (Ganguly et al., 1998).

Garnets with convex-upward  $REE_N$  patterns, i.e. the symplectite type varieties (Classes 2 and 5), normalized to J4 garnet, have an extreme MREE hump at nearly 10 times primitive garnet and a strong decrease towards HREE (Fig. 10b). They are considered as a subtype of sinusoidal  $REE_N$  garnets described above. According to Ivanic et al. (2003), the very steep positive slope from LREE to MREE of these garnets is likely to have been produced by an evolved metasomatic fluid or melt with  $Sm_N/Lu_N \gg 1$  and with  $Sm_N/La_N \leq 1$ . The authors suggest that the formation of such LREE-enriched melts may result from fractional crystallization where garnet itself plays the major role in generating the extreme LREE enrichment over HREE because of its widely varying partition coefficients.

## 6.2. Stage 2: N-type garnet formation

Figure 10c illustrates that the N-type varieties, i.e. the bulk of the xenolith-hosted, lherzolitic and megacryst classes, are closest to the primitive J4 garnet composition in terms of REE contents. Based on subparallel chondrite-normalized whole rock REE patterns and variable  $Al_2O_3$  contents of the garnet facies peridotite xenoliths, Peltonen et al. (1999) concluded that these rocks originally formed as ultramafic cumulates from mafic-ultramafic melts with broadly chondritic REE distribution (E-MORB). These cumulates could represent early Proterozoic oceanic lithosphere, tectonically subducted and now underplating the craton margin, and/or younger asthenospheric additions to the base of the lithosphere. Another monitor of mantle fertility is the Cr content of mantle garnets that is mainly controlled by the level of major element depletion in the host peridotite (Griffin et al., 1999a, 1999b). Indeed, the "primitive" REE profiles of the lherzolitic garnet varieties (Fig. 10c) with con-

tradictory depleted major element chemistries (e.g.  $Cr_2O_3 > 4$  wt%) are not considered as a primary feature but may have also resulted from metasomatic re-enrichment (Griffin et al., 1989b, Stachel et al., 1998), such as infiltration of the Archean mantle by a metasomatic melt close in composition to megacryst-forming magma (Burgess & Harte, 2004). There are some considerations that favor the idea of re-fertilization in the Kaavi-Kuopio mantle section. The Y-Zr classification (Fig. 7) indicates melt metasomatism. The Ti contents of the garnets from the garnet facies peridotite xenoliths and the N-type garnet xenocrysts classified as lherzolitic/wehrlitic types are clearly elevated ( $TiO_2$  up to 0.89 wt% and 1.01 wt%, respectively) and, moreover, their REE contents are identical to those of the megacryst composition pyropes (Figs. 8a, e-g). Although few in number, the existence of high-temperature Ti-poor lherzolitic grains with sinusoidal  $REE_N$  profiles (Fig. 8f) is extremely significant for the hypothesis of melt metasomatism. The latter type of garnet xenocrysts possibly originated from remnants of depleted material that was once predominant at depths greater than 180 km but that was virtually destroyed by re-fertilization as evidenced by the abundance of Ti-rich pyropes. This MREE, HREE and Ti enrichment event did not affect these rare depleted high-T lherzolitic grains nor the medium-T subcalcic harzburgitic (Fig. 8d) and Ti-poor lherzolitic varieties (Fig. 8e). Lower LREE concentrations in lherzolitic garnets compared to harzburgitic grains may be a consequence of the redistribution of REE during re-equilibration with Cpx (Stachel et al., 1998). Wang (1998), for example, has demonstrated that the Cpx/garnet partition coefficient for Ce is 2.91 and for Yb 0.02.

## 6.3. Stage 3: CCGE garnet formation

Kopylova et al. (2000) suggested that Ca-saturated Cpx-bearing garnet-spinel cratonic peridotites that host CCGE garnets are restricted to extraordinary mantle segments, since garnet and spinel-bearing mantle is usually too depleted to provide sufficient Cpx for development of the CCGE trend. The rari-

ty of the trend may also derive from the disequilibrium between phases in cratonic spinel-garnet peridotites (Kopylova et al., 2000; Smith & Boyd, 1992). In the Kaavi-Kuopio mantle segment CCGE garnets are hosted by garnet-spinel harzburgites containing minor amounts (<5 %) of Cpx. In the xenoliths CCGE garnets exhibit an irregular and amoeboidal texture that is very different from the rounded appearance of garnets in the garnet facies peridotite xenoliths (Peltonen et al., 1999). The amoeboid texture of the CCGE assemblages is typical of spinel-garnet-pyroxene intergrowths, which represent equilibrium textures in low-T peridotite xenoliths (Ionov et al., 1993; Field & Haggerty, 1994).

The ultra-depletion of CCGE garnets with respect to Ti, Y, Zr and REE (Figs. 6, 7, 10D) combined with their contradictory saturation in Ca, indicate that their host-peridotite has experienced a multi-stage history of depletion and enrichment events. The distinct positive slope of CCGE garnets in HREE from Dy/Er to Lu (Figs. 8b and 10d) has been interpreted elsewhere to represent a memory of an ancient melt extraction event that affected the primitive mantle source (Stachel et al., 1998). According to Kopylova et al. (2000) CCGE garnets may originate from an ultra-depleted mantle that has been later re-fertilized in Ca by some chemical enrichment process. The excess Ca has led to the crystallization of secondary Cpx and the transformation of harzburgitic garnets to lherzolitic, similar to that described from mantle garnets from suites in Kimberley, South Africa (Schulze, 1995; Griffin et al., 1999b). Interestingly, the proposed enrichment process has not fertilized the trace element contents of the garnets or affected their REE contents. Moreover, the whole rock analyses of the rare Kaavi-Kuopio garnet-spinel facies peridotite xenoliths show that, in fact, they contain less CaO than the other peridotitic xenolith varieties, 0.19–0.92 wt% vs. 0.72–1.55 wt%, respectively (Peltonen et al., 1999).

Peltonen et al. (1999) concluded that the low-T garnet-spinel peridotites could represent harzburgitic residues, i.e., remnants of the reworked Archean lithosphere, metasomatized shortly before or during invasion by a kimberlite-derived melt or fluid complete-

ly obscuring their ancient isotopic signature. Carbone & Canil (2002) suggested based on the Slave craton examples that this enrichment event could have been carbonatite metasomatism, where Cpx forms from Opx as a result of the interaction of carbonate melt with harzburgite (Yaxley et al., 1998). However, neither of these events would likely preserve the ultra-depleted nature of CCGE garnets with respect to trace elements, since the distribution of trace elements among all minerals in a peridotite will control the signature of garnet. Overall, the trace element budget for garnet-bearing peridotites is dominated by both Cpx and garnet (Glaser et al., 1999; Schmidberger & Francis, 2001). An intriguing possibility is that the shallow (<110 km) CCGE garnet bearing mantle layer has been somehow affected or modified by events connected to the Svecofennian orogeny, since this layer is not observed further into the Karelian craton based on mantle xenocryst studies from the Kuhmo area kimberlites (O'Brien et al., 2003).

## 7. Conclusions

The REE contents of the Kaavi-Kuopio mantle-derived garnet xenocryst bear evidence of an extensive ancient melt extraction event, similar to observations from lithosphere underlying Archean cratons elsewhere. The highly depleted lithosphere was subsequently affected by fluid metasomatism involving introduction of a fractionated fluid/melt low in HREE giving rise to the sinusoidal REE<sub>N</sub> patterns, characteristic for subcalcic harzburgitic garnets worldwide. Lherzolitic garnets, forming N-type REE patterns, document an enrichment event of MREE and HREE probably by metasomatism by silicate melts that also imprinted a Ti-overprint on most of the pyrope garnets. Harzburgitic and rare lherzolitic garnets have remained unaffected in zones or layers by this metasomatic event. Lower LREE concentrations in lherzolitic garnets compared to harzburgitic varieties may be a function of the redistribution of REE during re-equilibration with Cpx.

The results from this study are consistent with the previous work that distinguished three layers in the

lithospheric mantle underlying Kaavi-Kuopio terrain. The subcalcic harzburgitic garnets forming sinusoidal REE<sub>N</sub> patterns do not occur at temperatures ( $T_{Ni}$ ) higher than 1150°C, i.e. at depths greater than 175 km. Garnets originating from the deepest layer of the lithosphere (>175 km) are mostly Ti-rich megacryst and lherzolitic garnets, but there are also a few lherzolitic grains depleted in Ti, Y and Zr, and with sinusoidal REE<sub>N</sub>. These rare grains, as well as the more frequent depleted grains from the 110–175 km horizon, assumingly represent depleted mantle material that escaped the melt metasomatic event resulting in the formation of abundant Ti-rich garnets. The probably multi-stage history of the shallowest mantle layer (<110 km) consisting of garnet-spinel-harzburgite and characterized by CCGE garnets remains an open research topic.

### Acknowledgements

This study was funded by the Geological Survey of Finland and the Academy of Finland. Prof. John Gurney and Dr. Andreas Späth from the University of Cape Town are thanked for the access to the LA-ICP-MS. Dr. Hugh O'Brien and an anonymous reviewer are appreciated for revising the manuscript and providing valuable suggestions for improvements. I am also grateful to the Editor-in-Chief, Dr. Petri Peltonen, for many great ideas. Mr. Bo Johanson and Mr. Lassi Pakkanen from the GTK E-beam Laboratory provided the micro analytical data. The GTK Research Laboratory, Dr. Jukka Marmo (head) and the laboratory personnel, are thanked for the support. The backup of professor Ilmari Haapala from the University of Helsinki is appreciated.

### References

- Burgess, S.R. & Harte, B., 2004. Tracing Lithosphere Evolution through the Analysis of Heterogeneous G9–G10 Garnets in Peridotite Xenoliths, II: REE Chemistry. *Journal of Petrology* 45, 609–633.
- Canil, D., 1991. Experimental evidence for the exsolution of cratonic peridotite from high-temperature harzburgite. *Earth and Planetary Science Letters* 106, 64–72.
- Canil, D., Schulze, D.J., Hall, D., Hearn, B.C. & Milliken, S.M., 2003. Lithospheric roots beneath western Laurentia: the geochemical signal in mantle garnets. *Canadian Journal of Earth Sciences* 40, 1027–1051.
- Carbno, G.B. & Canil, D., 2002. Mantle structure beneath the SW Slave Craton, Canada: Constraints from Garnet Geochemistry in the Drybones Bay kimberlite. *Journal of Petrology* 43, 129–142.
- Field, S.W. & Haggerty, S.E., 1994. Symplectites in upper mantle peridotites: development and implications for the growth of subsolidus garnet, pyroxene and spinel. *Contributions to Mineralogy and Petrology* 118, 138–156.
- Ganguly, J., Tirone, M. & Hervig, R.L., 1998. Diffusion kinetics of samarium and neodymium in garnet, and a method for determining cooling rates of rocks. *Science* 281, 805–807.
- Glaser, S., Foley, S.F. & Gunther, D., 1999. Trace element compositions of minerals in garnet and spinel peridotite xenoliths from the Vitim volcanic field, Transbaikalia, eastern Siberia. *Lithos* 48, 263–285.
- Green, T.H., 1980. Island arc and continent-building magmatism – A review of petrogenic models based on experimental petrology and geochemistry. *Tectonophysics* 63, 367–385.
- Grégoire, M., Bell, D.R. & le Roex, A.P., 2003. Garnet lherzolites from the Kaapvaal Craton (South Africa): Trace element evidence for a metasomatic history. *Journal of Petrology* 44, 629–657.
- Griffin, W.L. & Ryan, C.G., 1995. Trace elements in indicator minerals: area selection and target evaluation in diamond exploration. In: W.L. Griffin (Ed.), *Diamond Exploration: Into the 21<sup>st</sup> Century*. *Journal of Geochemical Exploration* 53, 311–337.
- Griffin, W.L., Cousens, D.R., Ryan, C.G., Sie, S.H. & Suter, G.F., 1989a. Ni in chrome pyrope garnets: A new geothermometer. *Contributions to Mineralogy and Petrology* 103, 199–202.
- Griffin, W.L., Smith, D., Boyd, F.R., Cousens, D.R., Ryan, C.G., Sie, S.H. & Suter, G.F., 1989b. Trace element zoning in garnets from sheared mantle xenoliths. *Geochimica et Cosmochimica Acta* 53, 561–567.
- Griffin, W.L., Fisher, N.I., Friedman, J., Ryan, C.G. & O'Reilly, S.Y., 1999a. Cr-pyrope garnets in the lithospheric mantle. I. Compositional systematics and relations to tectonic setting. *Journal of Petrology* 40, 679–704.
- Griffin, W.L., Shee, S.R., Ryan, C.G., Win, T.T. & Wyatt, B.A., 1999b. Harzburgite to lherzolite and back again: metasomatic processes in ultramafic xenoliths from the Wesselton kimberlite, Kimberley, South Africa. *Contributions to Mineralogy and Petrology* 134, 232–250.
- Gurney, J.J., 1984. A correlation between garnets and diamonds. In: Glover, J.E. & Harris, P.G., (eds.) *Kimberlite occurrence and origin: A basis for conceptual models in exploration*. Geol. Dept. and Univ. Ext., University of Western Australia, Publication 8, 143–166.
- Hoal, K.E.O., Hoal, B.G., Erlank, A.J. & Shimizu, N., 1994. Metasomatism of the mantle lithosphere recorded by rare earth elements in garnets. *Earth and Planetary Science Letters* 126, 303–313.

- Ionov, D.A., Ashchepkov, I.V., Stosch, H.-G., Witt-Eickchen, G. & Seck, H.A., 1993. Garnet peridotite xenoliths from the Vitim volcanic field, Baikal region: the nature of the garnet-spinel peridotite transition zone in the continental mantle. *Journal of Petrology* 34, 1141–1145.
- Ivanic, T., Harte, B., Burgess, S., Gurney, J., 2003. Factors in the formation of sinuous and humped REE patterns in garnet from mantle harzburgite assemblages. In: Extended abstracts. 8<sup>th</sup> International Kimberlite Conference, Victoria, BC, Canada, 5pp.
- Kontinen, A., Paavola, J. & Lukkarinen, H., 1992. K-Ar ages of hornblende and biotite from Late Archean rocks of eastern Finland; interpretation and discussion of tectonic implications. *Geological Survey of Finland, Bulletin* 365, 31 p.
- Kopylova, M.G., Russell, J.K. & Cookenboo, H., 1999. Petrology of peridotite and pyroxenite xenoliths from the Jericho kimberlite: Implications for the thermal state of the mantle beneath the Slave Craton, northern Canada. *Journal of Petrology* 40, 79–104.
- Kopylova, M.G., Russell, J.K., Stanley, C. & Cookenboo, H., 2000. Garnet from Cr- and Ca-saturated mantle: implications for diamond exploration. *Journal of Geochemical Exploration* 68, 183–199.
- Kukkonen, I.T. & Peltonen, P., 1999. Xenolith controlled geotherm for the central Fennoscandian Shield: Implications for lithosphere–asthenosphere relations. *Tectonophysics* 304, 301–315.
- Kukkonen, I.T., Kinnunen, K.A. & Peltonen, P., 2003. Mantle xenoliths and thick lithosphere in the Fennoscandian Shield. *Physics and Chemistry of the Earth* 28, 349–360.
- Lehtonen, M.L., O'Brien, H.E., Peltonen, P., Johanson, B.S. & Pakkanen, L.K., 2004. Layered mantle at the Karelian Craton margin: P-T of mantle xenocrysts and xenoliths from the Kaavi-Kuopio kimberlites, Finland. *Lithos* 77, 593–608.
- Lehtonen, M.L., Pakkanen, L.K. & Johanson, B.S., 2005. Electron microprobe and LA-ICP-MS analyses of garnet xenocrysts from Kaavi-Kuopio area kimberlites. *Geological Survey of Finland, Open file report M 41.2/2005/1*.
- McDonough, W.F., Sun, S.S., 1995. The composition of the Earth. *Chemical Geology* 120, 223–253.
- Nixon, P.H., van Calsteren, P.W.C., Boyd, F.R. & Hawkesworth, C.J., 1987. Harzburgites with diamond facies from southern African kimberlites. In: Nixon, P.H. (ed.) *Mantle Xenoliths*, John Wiley & Sons Ltd., xxx p.
- O'Brien, H.E., Lehtonen, M.L., Spencer, R.G. & Birnie, A.C., 2003. Lithospheric mantle in eastern Finland: 250 km 3D transect. In: Extended abstracts, 8<sup>th</sup> International Kimberlite Conference, Victoria, BC, Canada, 5pp.
- O'Brien, H.E., Peltonen, P. & Vartiainen, H., 2005. Kimberlites, carbonatites and alkaline rocks. In: Lehtinen, M. et al. (eds.) *Precambrian geology of Finland – Key to the evolution of the Fennoscandian Shield*. Elsevier Science B.V., Amsterdam, xxx-yyy
- O'Brien, H.E. & Tyni, M., 1999. Mineralogy and Geochemistry of Kimberlites and Related Rocks from Finland. In: Gurney, J.J. et al., (eds.) *Proceedings of the 7<sup>th</sup> International Kimberlite Conference*, Cape Town, South Africa, Vol. 2, 625–636.
- O'Neill, H.S.C. & Wood, B.J., 1979. An experimental study of the iron-magnesium partitioning between garnet and olivine and its calibration as a geothermometer. *Contributions to Mineralogy and Petrology* 70, 59–70.
- Pearson, D.G., 1999. The age of continental roots. *Lithos* 48, 171–194.
- Pearson, N.J., Griffin, W.L., Kaminsky, F.V., van Achterbergh, E. & O'Reilly, S.Y., 1998. Trace element discrimination of garnet from diamondiferous kimberlites and lamproites. In: Extended abstracts, 7<sup>th</sup> International Kimberlite Conference, Cape Town, South Africa, 673–675.
- Peltonen, P., 1999. Silicification of garnet peridotite xenoliths from the Lahtojoki kimberlite pipe, Finland. In: Gurney, J.J. et al., (eds.) *Proceedings of the 7<sup>th</sup> International Kimberlite Conference*, Cape Town, South Africa, Vol. 2, 659–663.
- Peltonen, P. & Mänttari, I., 2001. An ion microprobe U-Th-Pb study of zircon xenocrysts from the Lahtojoki kimberlite pipe, eastern Finland. *Bulletin of the Geological Society of Finland* 73, 47–58.
- Peltonen, P. & Brüggemann, G., submitted. Origin of layered continental mantle (Karelian craton, Finland): Geochemical and Re-Os isotope constraints. *Lithos*.
- Peltonen, P., Huhma, H., Tyni, M. & Shimizu, N., 1999. Garnet peridotite xenoliths from kimberlites of Finland: Nature of the continental mantle at an Archean craton – Proterozoic mobile belt transition. In: Gurney, J.J. et al., (eds.) *Proceedings of the 7<sup>th</sup> International Kimberlite Conference*, Cape Town, South Africa, Vol. 2, 664–675.
- Peltonen, P., Kinnunen, K. A. & Huhma, H., 2002. Petrology of two diamondiferous eclogite xenoliths from the Lahtojoki kimberlite pipe, eastern Finland. *Lithos* 63, 151–164.
- Robinson, B.W. & Graham, J., 1992. Advances in Electron Microprobe Trace Element Analysis. *Journal of Computer-Assisted Microscopy* 4, 263–265.
- Ryan, C.G., Griffin, W.L. & Pearson, N.J., 1996. Garnet geotherms: Pressure-temperature data from Cr-pyroxene garnet xenocrysts in volcanic rocks. *Journal of Geophysical Research* 101, 5611–5625.
- Saltzer, R.L., Chatterjee, N. & Grove, T.L., 2001. The spatial distribution of garnets and pyroxenes in mantle peridotites: Pressure-temperature history of peridotites from the Kaapvaal Craton. *Journal of Petrology* 42, 2215–2229.
- Schulze, D.J., 1995. Low-Ca garnet harzburgites from Kimberley, South Africa: abundance and bearing on the structure and evolution of the lithosphere. *Journal of Geophysical Research* 100, 513–526.



- Schulze, D.J., 2003. A classification scheme for mantle-derived garnets in kimberlite: a tool for investigating the mantle and exploring for diamonds. *Lithos* 71, 195–213.
- Schmidberger, S.S. & Francis, D., 2001. Constraints on the trace element composition of the Archean mantle root beneath Somerset Island, Arctic Canada. *Journal of Petrology* 42, 1095–1117.
- Shimizu, N., 1975. Rare earth elements in garnets and clinopyroxenes from garnet lherzolite nodules in kimberlites. *Earth and Planetary Science Letters* 25, 26–32.
- Shimizu, N. & Richardson, S.H., 1987. Trace element abundance patterns of garnet inclusions in peridotite-suite diamonds. *Geochimica et Cosmochimica Acta* 51, 755–758.
- Smith, D. & Boyd, F.R., 1992. Compositional zonation in garnets in peridotite xenoliths. *Contributions to Mineralogy and Petrology* 112, 134–147.
- Sobolev, N.V., Lavrentiev, Yu.G., Pokhilenko, N.P. & Us-ova, N.P., 1973. Chrome-rich garnets from the kimberlites of Yakutia and their paragenesis. *Contributions to Mineralogy and Petrology* 40, 39–52.
- Stachel, T., Harris, J.W., Tappert, R. & Brey, G.P., 2003. Peridotitic diamonds from the Slave and the Kaapvaal cratons – similarities and differences based on a preliminary data set. *Lithos* 71, 489–503.
- Stachel, T., Viljoen, K.S., Brey, G. & Harris, J.W., 1998. Metasomatic processes in lherzolitic and harzburgitic domains of diamondiferous lithospheric mantle: REE in garnets from xenoliths and inclusions in diamonds. *Earth and Planetary Science Letters* 159, 1–12.
- Stachel, T., Viljoen, K.S., McDade, P. & Harris, J.W., 2004. Diamondiferous lithospheric roots along the western margin of the Kalahari Craton – the peridotitic inclusion suite in diamonds from Orapa and Jwaneng. *Contributions to Mineralogy and Petrology* 147, 32–47.
- Tyni, M., 1997. Diamond prospecting in Finland – a review. In: Papunen H. (ed.) *Mineral deposits: research and exploration, where do they meet?* Proceedings of the 4<sup>th</sup> SGA Meeting, Rotterdam, A.A. Balkema, 789–791.
- Wang, W., 1998. Formation of diamond with mineral inclusions of “mixed” eclogite and peridotite paragenesis. *Earth and Planetary Science Letters* 160, 831–843.
- Woodland, A. B. & Peltonen, P., 1999. Ferric iron contents of garnet and clinopyroxene and estimated oxygen fugacities of peridotite xenoliths from the Eastern Finland Kimberlite Province. In: Gurney, J.J. et al., (eds.) *Proceedings of the 7<sup>th</sup> International Kimberlite Conference, Cape Town, South Africa, Vol. 2*, 904–911.
- Yaxley, G.M., Green, D.H. & Kamenetsky, V., 1998. Carbonatite metasomatism in the southeastern Australian lithosphere. *Journal of Petrology* 39, 1917–1930.